Materials Science in Semiconductor Processing 124 (2021) 105596

Contents lists available at ScienceDirect

Materials Science in Semiconductor Processing

journal homepage: http://www.elsevier.com/locate/mssp

Reactive ion etching of PbSe thin films in $CH_4/H_2/Ar$ plasma atmosphere

Gang Yang [a,*], Binbin Weng [a,b,**]

[a] Microfabrication Research and Education Center, University of Oklahoma, Norman, OK73019, USA
[b] School of Electrical and Computer Engineering, University of Oklahoma, Norman, OK73019, USA

ARTICLE INFO

Keywords:
Reactive ion etching
Lead selenide
Narrow bandgap semiconductor

ABSTRACT

In this work, we reported a reactive ion etching of PbSe thin films on silicon in $CH_4/H_2/Ar$ plasma atmosphere. Various etching parameters that affect dc self-bias, the etching rate and the etching smoothness of the surface and sidewalls, including rf power, gas ratio, and process pressure, have been systematically investigated. It is found that the dc self-bias has an approximate linear relationship with rf power, but it decreases as the process pressure increases. The etching rate increases with increasing rf power and decreasing process pressure. Additionally, the etching rate increases to the maximum as CH_4 percentage increases to 40%, beyond which it decreases with further increasing CH_4 percentage due to formation of polymer. Furthermore, SEM results show that for all investigated samples except one etched in atmosphere with 60% CH_4, the etched surfaces are smooth, and the sidewalls are vertical. The etched profile of sample etched in atmosphere with 60% CH_4 is very rough, which should be attributed to formation of polymer as well.

1. Introduction

Mid-infrared (Mid-IR) semiconductors are functional materials with bandgaps smaller than ~ 0.4 eV. Their popular applications mainly include thermal imaging, thermoelectric energy conversion and so on. Among them, lead selenide (PbSe) is one of the most popular candidates to fabricate solid-state devices such as mid-IR light-emitting diodes, laser, detectors, thermoelectric coolers and power generators [1–12]. To fabricate such devices, lithographic patterning followed by the etching process are the essential steps to take. Although wet chemical etching is the simple and straightforward method for etching and structuring the device mesa, with the increasing demand of manufacturing device arrays of small pixels, close pitch and high density features, the lateral and isotropic etching issues of wet etching process make it unable to satisfy new requirements as mentioned. In contrast to the wet etching, plasmonic assisted dry etching processes has drawn more and more attentions mostly due to their better aspect-ratio anisotropic etching advantage.

For the plasma dry etching process, a desired etching profile should include low physical damage, high selectivity, and smooth etched surface and sidewalls, considering their strong influence on the device performance such as electric leakage and optical loss [13,14]. Thus, significant efforts including plasma gas phase selection, optimization of reactive ion etching (RIE) power or inductively coupled plasma (ICP) power, and chamber pressure to date has been carried out with the aforementioned purpose [2,14–16]. CH_4/H_2-based plasma dry etching is well established in the reactive ion etching, which has been proven to cause the least damage in III-V semiconductors such as InP, GaInAs, GaAs, AlGaAs [17] and II-VI semiconductors such as ZnTe, ZnSe, CdS [18]. In CH_4/H_2 gas phase plasma chemistry for room-temperature dry etching of III-V compound semiconductors, the role of CH_4 is to form volatile metal organic species which are easily removed from sample surface by ion sputtering, while H_2 forms volatile hydride species with group V elements [16,19–21]. Lee et al. [16] reported the etching results of GaAs, AlGaAs, GaSb, and GaP in different ICP plasma chemistries, i.e. pure Ar, $CH_4/H_2/Ar$ and $CH_4/H_2/N_2$. They found that dc bias on the rf chuck decreased exponentially with increasing ICP power and the etching rate showed a little dependence on the chamber pressure in $CH_4/H_2/Ar$. In contrast, Yu et al. [22] found a high process pressure increased the etching rate due to the increase of the radical density and the surface roughness decreased as the process pressure increased. Etrillard et al. [23] reported less sidewall damage on InP features etched in $CH_4/H_2/O_2$ ICP discharges than with comparable RIE plasma. Zhao et al. [15] reported that an increase in temperature can greatly improve the surface roughness and sidewall verticality. Jiao et al. [14] found that a higher process pressure and higher CH_4 fraction in CH_4/H_2 resulted in

* Corresponding author. Microfabrication Research and Education Center, University of Oklahoma, Norman, OK73019, USA.
** Corresponding author. Microfabrication Research and Education Center, University of Oklahoma, Norman, OK73019, USA.
E-mail addresses: gang.yang-1@ou.edu (G. Yang), binbinweng@ou.edu (B. Weng).

https://doi.org/10.1016/j.mssp.2020.105596
Received 20 April 2020; Received in revised form 16 November 2020; Accepted 25 November 2020
Available online 8 December 2020

a smoother etched surface.

Although a lot of works on the plasma dry etching on II-VI and III-V semiconductors has been reported, there has been few data available on IV-VI semiconductors. So far, there is only one report from Schwarzl et al. [2] back in 1990. With the technology advancement in the past 30 year and newly emerging challenges of IV-VI's materials and devices, a new study to systematically investigate the etching procedure of this special material is highly desired. In this work, we present the dry etching of PbSe thin film on silicon in $CH_4/H_2/Ar$ plasma atmosphere by the reactive ion etching (RIE) technique. We introduced physical etching by adding ionic argon gas to chemical etching process of CH_4/H_2 plasma, investigated the influences of RIE power, gas ratio and process pressure on the dc self-bias, etching rate, profile of etched surface and verticality of sidewalls, and developed an optimized combination of etching parameters for achieving high quality etching results on PbSe films.

2. Experimental details

The samples used in the RIE experiments are PbSe layers with a thickness of 1.2 μm, which were grown on silicon substrates by the magnetron sputtering technique. In order to make samples clean for photolithography, the samples were washed in acetone at 55 °C and in methanol at room temperature for 15 min and 5 min, respectively, then were immersed in a mixture solution of de-ionized water, ammonium hydroxide and hydrogen peroxide for further cleaning at 65 °C for 10 min. Prior to RIE, all of the cleaned samples were patterned with 2 μm thick photoresist (AZ5214). The photoresist patterning was conducted under MJB3 mask aligner (Suss, Germany). The RIE experiments were performed in Trion ICP-RIE plasma etching system (Trion Technology, USA). The samples were placed in the center of the reactor chamber, which was then pumped down to less than 1.5×10^{-5} Torr. The RIE experiments were carried out in $CH_4/H_2/Ar$ plasma atmosphere. The gas flow rates through the reactor were controlled by mass flow controllers. The process pressure was adjusted by a control valve connected to the vacuum pump. All process parameters were controlled by a computer. After the etching, all samples were characterized. The etching depth was measured by KLA Tencor profilometer (KLA Corporation, California, USA). The etched profiles of all samples were examined by a JSM-6060 scanning electron microscope (SEM) (JEOL, Japan). SEM images were taken by rotating sample holder at counter clockwise (CCW) to reach a 60° tilt angle to examine etched profiles. Additionally, a SEM image of the cross-section surface of the etched sample was taken to investigate verticality of the etched sidewall of sample.

3. Results and discussion

3.1. dc self-bias voltage

As we know, the dc self-bias is a negative potential on the power electrode, which is a result of the impinging of electrons on the power electrode. The factors that affect dc-self bias voltage are: ratio between the surface areas of the ground and power electrodes which should be invariable for a certain RIE equipment, process pressure being inversely proportional to dc-self bias, rf power and type of gas. RIE rf power is a significant influential factor on the etching rate and etched profile by applying a direct impact on dc-self bias voltage on the electrode. The dependences of self-bias on rf power for the investigated samples are shown in Fig. 1.

It is found that the dc self-bias voltage increases approximate linearly as rf power increase. In the circumstance that all above impact factors are invariable except rf power, we can assume that the relationship between ion current (or ion flux) and dc-self bias are written as [16]:

$$P_{rf} = V_{dc\ bias} \times I_{ion} \quad (1)$$

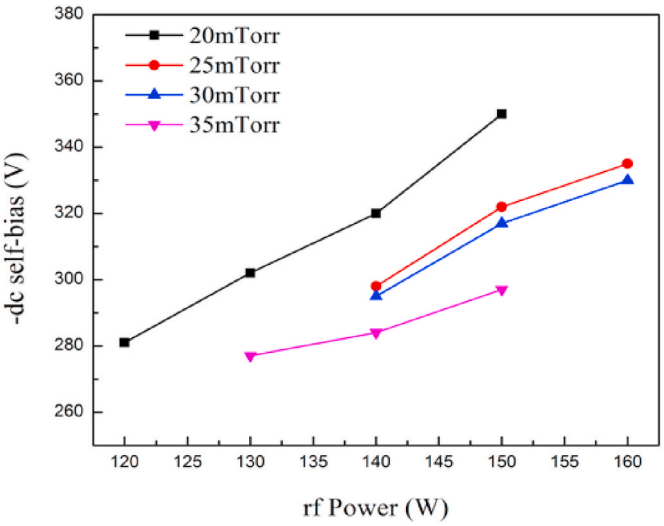

Fig. 1. dc Bias as a function of rf power at different process pressures with a gas mixture of $10CH_4/10H_2/5Ar$.

where P_{rf} is applied rf power on the power electrode, $V_{dc\ bias}$ is dc-self bias voltage on the power electrode and I_{ion} is the ion current or flux from the plasma. Thus, the rf power has a proportional influence on the dc self-bias. However, this proportionality may vary due to a change in the process pressure, which can be verified by Fig. 1, Fig. 2(a) and (b). Fig. 2(a) shows the relationship between dc self-bias voltage and process pressure with a gas mixture of $10CH_4/10H_2/Ar$ at 150W rf power, while Fig. 2(b) describes this relationship with a gas mixture of $8CH_4/8H_2/Ar$ at 200W rf power. All three figures show that dc self-bias voltage has a decreasing trend with an increase in the process pressure. The influence of the process pressure on the dc self-bias can be interpreted as below. As the process pressure increases, the mean free path of the electrons decreases, so the collision probability between particles increases. The more collisions between particles lead to more recombination of ions and electrons, so the number of free electrons and ions arriving at sample chuck decreases [16]. Therefore, the dc self-bias voltage decreases.

3.2. Etching rate

Both Fig. 2(a) and (b) show that the etching rate decreases with increasing process pressure, while it increases as rf power increases shown in Fig. 3.

The $CH_4/H_2/Ar$ plasma contains active species, such as electrons, argon ions Ar^+, radical CH_x (x = 1,2,3) and hydrogen atom [24–28]. The etching process caused by these reactive species consists of two etching components: physical and chemical etchings. The bombardment of argon ions on sample surface contributes to the physical etching component, while the chemistry etching component is attributed to the chemical reactions of radical CH_x and H with PbSe layer, which could produce various volatile lead- and selenium-containing byproducts. These volatile products are pumped out by the vacuum pump. Lead-containing byproducts could be a kind of lead hydrocarbon compound and selenium-containing products could be H_2Se. Eddy et al. [26] identified the existence of H_2Se as a volatile product in etching of ZnSe in $CH_4/H_2/Ar$ plasma atmosphere using an in-situ mass spectroscopy connected to plasma etching system. However, a further work will be needed to justify the existence of volatile lead hydrocarbons compound and H_2Se in etching process of PbSe compound in $CH_4/H_2/Ar$ plasma atmosphere in future.

The etching rate is dependent upon both physical and chemical etching components. The increase in rf power results in an increase in the plasma density and therefore increasing the number of reactive

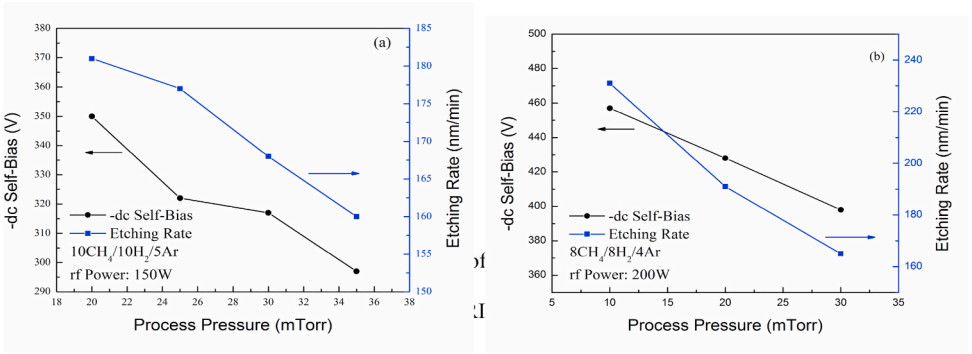

Fig. 2. Etching rate and dc bias as a function of process pressure (a) at 150W RIE power with a mixture of $10CH_4/10H_2/5Ar$, and (b) at 200W RIE power with a mixture of $8CH_4/8H_2/4Ar$.

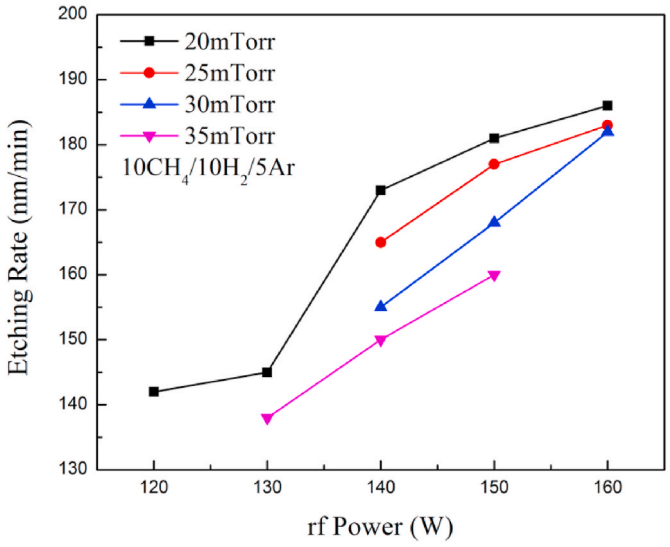

Fig. 3. Etching rate as a function of RIE power at different process pressures with a gas mixture of $10CH_4/10H_2/5Ar$.

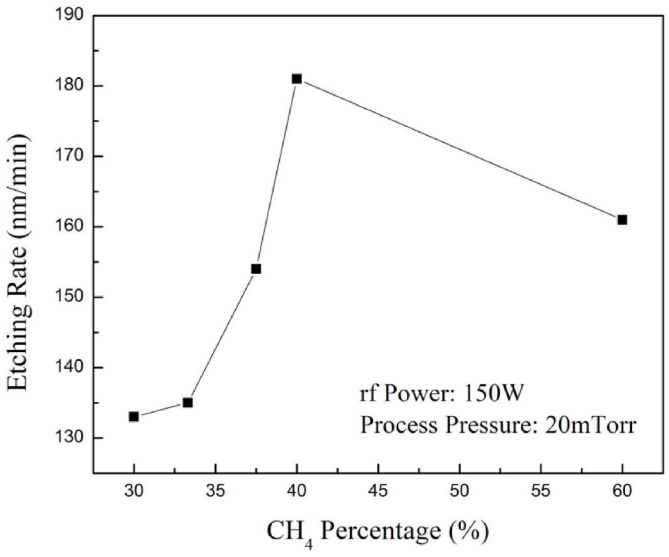

Fig 4. Influences of CH_4 percentage on the etching rates at 150 W and 20 mTorr pressure.

radicals and argon ions, which not only accelerates physical etching but chemical etching as well. Therefore, the etching rate increases with increasing rf power. In contrast, at higher process pressure, since a decrease in the mean free path of electrons and ions may result in a recombination of electrons and ions, the electron density may decrease significantly, which further causes a decrease in both dissociation rate and radical density. Thus, increasing process pressure reduces both physical and chemical etching components and therefore a decrease in the etching rate. Oda et al. [29] investigated the influences of the chamber pressure on the density of radical neutrals in CH_4/H_2 plasma and found that with increasing chamber pressure, small species such as CH_3 and CH_2 radical density decreased, while large species, i. e. C_2H_5 radical density increased. Based on Oda et al.'s findings [29], a decrease in chemical etching component with increasing process pressure should indicate an existence of CH_x (x = 1, 2, 3) radicals in the present work. Furthermore, in CH_4/H_2-based etching chemistry, there is a micro-masking due to excessive polymer deposition [2,14], which may be another factor leading to a decrease in the etching rate as the chamber pressure increases.

Since the polymer formation is strongly dependent on content of C–H chains, we have further investigated the influence of CH_4 percentage $CH_4/H_2/Ar$ atmosphere on the etching rate. In the experiments, the rf power was set at 150W and the chamber pressure was at 20mTorr. The measured etching rates are shown in Fig. 4. It is found that as CH_4 percentage increases, the etching rate initially increases to reach the maximum at 40% of CH_4 percentage, then declines. This result show that the etching takes a dominant role when CH_4 percentage is less than 40%, while the polymer formation takes a dominant role when CH_4 percentage is more than 40%. The best etching parameter group is $10CH_4/10H_2/5Ar$ with 150 W rf power at a process pressure of 20mTorr. These results should be attributed to contribution from more chemical etching.

3.3. Characterization of etched profiles

In order to examine the surface profiles of the etched samples, we used SEM to examine the etched profiles and sidewalls of all samples. Fig. 5(a), (b), (c), (d) and (e) show the SEM images of the etched surfaces of samples etched in different CH_4 percentage atmospheres. It is found that except sample etched in 60% CH_4 atmosphere, all other samples have smooth etched surfaces, as shown in Fig. 5(a), (b), (c) and (d). Fig. 5(e) shows that the etched surface of sample etched in 60%CH_4 atmosphere is very rough, which should be also attributed to formation of polymer [14,28,30–32]. In the CH_4/H_2 RIE process, there is a competition between etching and formation of polymer in CH_4/H_2 plasma etching chemistry. H and CH_x (x = 1,2,3) radicals are generated in the plasma, helping etching process, meanwhile, CH_x (x = 1,2,3) radicals can react with each other to form polymer [14]. Ar in the mixture of $CH_4/H_2/Ar$ plasma atmosphere takes a major role in the physical etching component, additionally, it can control polymer formation. Jiao et al. [14] reported that CH_4/H_2 ratio has a significant

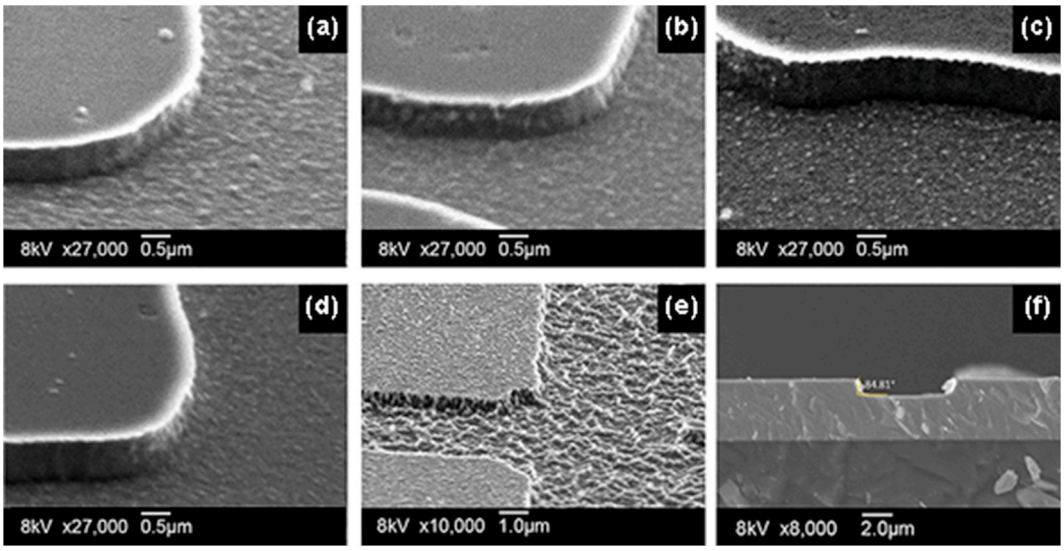

Fig. 5. SEM images of the samples etched in atmospheres with different CH_4 percentages at 20mTorr and 150W rf power, (a) 30%, (b) 33.3%, (c) 37.5%, (d) 40% and (e) 60%, and (f) SEM image of the cross-section of the sample with 40% CH_4.

influence on the surface smoothness since the formation of polymer is dominated by CH_4 fraction. M. Lysevych [33] suggested a preferable ratio of CH_4 and H_2 is between ½ and ¼. However, in our current experiments, three ratios of CH_4 and H_2 we used were 0.6, 1.0 and 3, which were all out of ¼ to ½. We found that the etched profile become very rough when CH_4/H_2 ratio was 3. Additionally, we found that compared to Fig. 5(d) and (a) shows a little rougher etched surface though less CH_4 fraction was used at the condition of (a). There could be a threshold value of CH_4 fraction for the competition between etching and formation of polymer. When CH_4 fraction is below the threshold value, CH_4 etching takes a dominant role in the competition and a higher CH_4 fraction resulted in a smoother etched surface [14], so Fig. 5(d) shows a smoother etched surface compared to the surface shown in Fig. 5(a). Contrarily, when CH_4 fraction is above the threshold value, the formation of polymer takes a dominant role in the competition so that the etched surface becomes very rough. Furthermore, we have also investigated the sidewalls using SEM observation of cross section surface of the sample etched in $10CH_4/10H_2/5Ar$ with a pressure of 20mTorr at 150W. It is found from Fig. 5(f) that the angle between the sidewall and etched surface is about 84.81, so the sidewalls are vertical.

4. Conclusions

In the present work, we have investigated RIE etching of PbSe thin film grown on the silicon substrate in $CH_4/H_2/Ar$ plasma. It was found that rf power, ratio of gas mixture and process pressure have significant influences on dc self-bias, the etching rate, smoothness of etched surface and sidewall verticality of the etched samples The dc self-bias voltage is approximately proportional to rf power, while it decreases with increasing process pressure. Similarly, the etching rate also increases with increasing rf power and decreasing process pressure. Additionally, the etching rate increases to the maximum as CH_4 percentage increases to 40%, beyond which it decreases with further increasing CH_4 percentage due to formation of polymer. Meanwhile, SEM results show that for the samples etched in all atmospheres except 60% CH_4, the etched surfaces are smooth, and the sidewalls are vertical, while with 60% CH_4, the etched surface is rough due to formation of polymer as well. Those results should be interpreted from the approaches of both physical and chemical etchings. These findings will be greatly helpful to fabrication of PbSe devices for the photonic application.

Author statement

The second and corresponding author took a supervision role. The first author conducted experiments and wrote manuscript.

Declaration of competing interest

The authors declare that they have no known competing financial interests or personal relationships that could have appeared to influence the work reported in this paper.

Acknowledgments

Authors would like to thank Preston R Larson for the support on the analysis of SEM results.

References

[1] L. Anicai, I. Sin, O. Brincoveanu, et al., Appl. Surf. Sci. 475 (2019) 803–812.
[2] T. Schwarzi, W. Heiß, G. Kocher-Oberlehner, G. Springholz, Semicond. Sci. Technol. 14 (1990) L11–L14.
[3] H. Yang, X.J. Li, G.D. Wang, J.B. Zheng, Coatings 444 (2018) 1–21, 8.
[4] X.G. Sun, K.W. Gao, X.L. Pang, H.S. Yang, A.A. Volinsky, Thin Solid Films 92 (2015) 59–68.
[5] W.J. Hu, S. Gao, P.N. Prasad, J.K. Wang, J. Xu, J. Nanomater. (2012) 183–190, 2012.
[6] H. Preier, Appl. Phys. 20 (1979) 189–206.
[7] J.M. Martin, J.L. Hernández, L. Adell, A. Rodriguez, F. López, Semicond. Sci. Technol. 11 (1996) 1740–1744.
[8] C. Gayner, K.K. Kar, W.C. Kim, Materials Today Energy 9 (2018) 359–376.
[9] B. Weng, J. Qiu, Z. Shi, Appl. Phys. B 123 (1) (2017). Article: 29.
[10] B. Weng, J. Ma, L. Wei, L. Li, J. Qiu, J. Xu, Z. Shi, Room temperature mid-infrared surface-emitting photonic crystal laser on silicon, Appl. Phys. Lett. 99 (22) (2011) 221110.
[11] J. Qiu, B. Weng, L.L. McDowell, Z. Shi, RSC Adv. 9 (72) (2019) 42516–42523.
[12] B. Weng, J. Qiu, Z. Yuan, P.R. Larson, G.W. Strout, Z. Shi, Appl. Phys. Lett. 104 (2) (2014), 021109.
[13] E. Gogolides, V. Constantoudis, G. Kokkoris, et al., J. Phys. Appl. Phys. 44 (2011) 174021.
[14] Y.Q. Jiao, T.D. Vries, R.-S. Unger, et al., J. Electrochem. Soc. 162 (8) (2015) E90–E95.
[15] X. Zhou, J.A. del Alamo, IEEE Electron. Device Lett. 35 (2014) 521–523.
[16] J.W. Lee, C.R. Abernathy, S.J. Pearton, et al., Plasma Sources Sci. Technol. 6 (1997) 499–507.
[17] L. Henry, C. Vaudry, Electron Letters, vol. 23, 1987, p. 1253.
[18] T. Matsui, H. Sugimoto, T. Ohishi, et al., Appl. Phys. Lett. 54 (1989) 1193–1194.
[19] M.A. Foad, C.D.W. Wilkinson, C. Dounscomb, R.H. Wiliams, Appl. Phys. Lett. 60 (1992) 2531–2533.
[20] S.J. Pearton, U.K. Chakrabarti, A. Perley, W.S. Hobson, J. Electrochem. Soc. 138 (1991) 1432–1439.

[21] R. Pereira, R. Jouckheere, M. Vanderssum, J. Vac. Sci. Technol. B 9 (1991) 1978.
[22] J.S. Yu, Y.T. Lee, Semicond. Sci. Technol. 17 (2002) 230–236.
[23] J. Etrillard, F. Heliot, P. Ossart, M. Juhel, G. Patriarche, P. Carcenac, C. Vieu, M. Puech, P. Maguin, J. Vac. Sci. Technol. 14 (1996) 1056.
[24] I.B. Denysenko, S. Xu, J.D. Long, P.P. Rutkevych, N.A. Azorenkov, K. Ostrikov, J. Appl. Phys. 95 (2004) 2713–2724.
[25] Y. Feurprier, Ch Cardinaud, B. Grolleau, G. Turban, Plasma Sources Sci. Technol. 6 (1997) 561–568.
[26] C.R. Eddy Jr., D. Leonhardt, V.A. Shamamian, J.E. Butler, J. Electron. Mater. 30 (2001) PP538–542.
[27] A.Z. Navilopulo, M.I. Mykyta, A.N. Mylymko, O.B. Shpenik, Atomic and Molecular Physics 53 (2013) 1251–1257.
[28] Annemie Bogaerts, Renaat Gijbels, Phys. Rev. 65 (2002) 15. PP0564021.
[29] A. Oda, Y. Suda, A. Okita, Thin Solid Films 516 (2008) 6570–6574.
[30] K. Ostrico, Plasma Nanoscience, Wiley-VCH Verlag GmbH & Co. KGaA, Germany, 2006, p. 484.
[31] M.A. Foad, D.W. Wilkinson, C. Dunscomb, R.H. Williams, Appl. Phys. Lett. 60 (20) (1992) 2531–2533.
[32] Y.-H. Ting, C.-C. Liu, S.-M. Park, H.Q. Jiang, P.F. Nealey, A.E. Wendt, Polymers 2 (2010) 649–663.
[33] M. Lysevych, H.H. Tan, F. Karouta, C. Jagadish, J. Electrochem. Soc. 158 (3) (2011) H281–H284.